International Journal of Climatology · RMetS

Characteristics of extreme daily precipitation events over the Canadian Arctic

Mark C. Serreze[1] | Jessica Voveris[1] | Andrew P. Barrett[1] | Shari Fox[1] |
Peter D. Blanken[2] | Alex Crawford[3]

[1]National Snow and Ice Data Center, Cooperative Institute for Research in Environmental Sciences, University of Colorado, Boulder, Colorado, USA

[2]Department of Geography, University of Colorado, Boulder, Colorado, USA

[3]Centre for Earth Observation Science, Department of Environment and Geography, University of Manitoba, Winnipeg, Manitoba, Canada

Correspondence
Mark C. Serreze, National Snow and Ice Data Center, Cooperative Institute for Research in Environmental Sciences, University of Colorado, Boulder, CO 80309, USA.
Email: mark.serreze@colorado.edu

Abstract

Given growing interest in extreme high-latitude weather events, we use records from nine meteorological stations and atmospheric reanalysis data to examine extreme daily precipitation events (leading, 99th and 95th percentile) over Arctic Canada. Leading events span 90 mm at Cape Dyer, along the southeast coast of Baffin Island, to 26 mm at Sachs Harbour, on the southwest coast of Banks Island. The 95th percentiles range from 20 to 30% of leading event sizes. Extreme events are most common on or near the month of climatological peak precipitation. Contrasting with Eurasian continental sites having a July precipitation peak corresponding to the seasonal peak in precipitable water, seasonal cycles in precipitation and the frequency of extremes over Arctic Canada are more varied, reflecting marine influences. At Cape Dyer and Clyde River, mean precipitation and the frequency of extremes peak in October when the atmosphere is quickly cooling, promoting strong evaporation from Baffin Bay. At all stations, leading events involved snowfall and strong winds and were associated with cyclone passages (mostly of relatively strong storms). They also involved strong vapour fluxes, sometimes associated with atmospheric rivers or their remnants. The most unusual sequence of events identified here occurred at Clyde River, where the three largest recorded precipitation events occurred in April of 1977. Obtaining first-hand accounts of this series of events has proven elusive. Identified links between extreme events and atmospheric rivers demonstrates the need to better understand how the characteristics of such features will change in the future.

KEYWORDS
Arctic, atmospheric rivers, Canada, cyclones, extremes, precipitation

1 | INTRODUCTION

Extreme precipitation events in the Arctic—recorded as snow, rain, or rain-on-snow—can have large impacts on Arctic ecosystems, wildlife, and human activities (Bjerke et al., 2015; Christensen et al., 2021). Rain-on-snow with subsequent re-freezing, occurring even in events with low precipitation amounts overall, have been linked to massive starvation-induced die offs of semidomesticated reindeer and musk oxen (Rennert et al., 2009; Forbes et al., 2016; Serreze et al., 2021). Large Arctic precipitation events have been linked to flooding, slush

avalanches and permafrost warming (Hansen *et al.*, 2014; Serreze *et al.*, 2015) as well as amplified melt and runoff from the Greenland Ice Sheet (Doyle *et al.*, 2015).

Results from numerous studies, taken together, describe a future Arctic with more precipitation, a transition from snowfall- to rainfall-dominated climates, and a shorter return period for high-intensity events (e.g., Kharin *et al.*, 2013; Sillmann *et al.*, 2013; Toreti *et al.*, 2013; Kusunoki *et al.*, 2015; McCrystall *et al.*, 2021; Dou *et al.*, 2022). However, as reviewed by Walsh *et al.* (2020), trend assessments of precipitation and precipitation extremes across the Arctic over the period of observations show no coherent pattern. Results reported in different studies depend on the time period and region examined and the type of analysis utilized with the research. Some studies relied on gauge records, while others relied on output from atmospheric reanalysis products. Most recently, Yu and Zhong (2021) examined trends in seasonal precipitation and extremes over the 1979–2016 period based on output from the ERA-Interim reanalysis. While more regions were found to have statistically significant positive (rather than negative) trends, especially in autumn and winter over the Arctic Ocean and the northern North Atlantic, negative trends were more the rule in areas of northern Eurasia and North America.

To provide context for interpreting projections of change from modelling studies (in addition to the mixed findings on trends from observational studies), it is useful to take a step back to get a better handle on the observed characteristics of extreme Arctic precipitation events. Here, we examine extreme precipitation events over the Canadian Arctic based on station data observations (nine stations with precipitation measurements spanning several decades) and atmospheric circulation fields from the European Centre for Medium Range Weather Forecasts (ECMWF) ERA5 atmospheric reanalysis. We focus on the largest (leading) events, along with those in the 99th and 95th percentile. How large are extreme precipitation events in the Canadian Arctic? What is their seasonality, bearing on whether they are associated with snow versus rain? What are the atmospheric circulation patterns that give rise to them? Are they commonly associated with atmospheric river events? Our study addresses these questions.

The approach is as follows: (a) select stations with long records of daily precipitation across the Canadian Arctic; (b) assess the size of extreme precipitation events and their geographical differences, focusing on the single largest event (leading event), 99th and 95th percentile events at each site; (c) assess the seasonality of extreme events in relation to the mean seasonal cycles of precipitation at each selected site and whether they fall as rain or snow; (d) look at the synoptic weather patterns associated with the largest (leading) events at each site and possible links with atmospheric rivers, narrow bands of high water vapour transport originating in the tropics or subtropics (Ralph and Dettinger, 2011; Ralph *et al.*, 2017); (e) examine April 1977 as a special case study, which contains the three largest events in the daily record for Clyde River, a small Inuit community that lies on the northeast coast of Baffin Island.

2 | DATA SOURCES

2.1 | Precipitation records

Daily records for Canadian meteorological stations were downloaded at https://climatedata.ca/download/#station-download. The records contain: total precipitation, total rainfall, total snowfall, the depth of snow on the ground, daily maximum, minimum and mean surface air temperature, wind speeds, heating degree days, and other variables. Quality flags are also provided. Not all stations contain all these variables, and some stations have a large amount of missing data. Canada is on the World Meteorological Organization's (WMO's) standard 06Z to 06Z Climate Day; the precipitation data are for the 24-hr period ending 06Z. Hence, an event reported (for example) on December 21 corresponds to the accumulated precipitation from 06Z December 21 to 06Z December 22.

We selected the nine stations across the Canadian Arctic (north of the Arctic circle) with the longest and most complete records (Figure 1 and Table 1). Station elevations range from 9 m (Hall Beach) to 393 m (Cape Dyer) above sea level. Some stations have undergone site re-locations through the years, and records are provided as separate files with different station names. The records may also overlap. For example, records for Clyde River (Baffin Island) are provided in files listed for CLYDE A, CLYDE RIVER A, and CLYDE RIVER CLIMATE, with slightly different geographical coordinates. In two cases (Hall Beach and Cambridge Bay), separate files were available under the same station name but span different time periods. Data from the most complete multiple records were combined into single records, using the longest records as the base to build from. Some records from automated stations were also available but were not used.

Daily precipitation in the Canadian network is measured to the nearest 0.2 mm for precipitation totals greater than 0.2 mm (see section 3.7 of MANOBS, https://www.canada.ca/content/dam/eccc/migration/main/manobs/73bc3152-e142-4aee-ac7d-cf30daff9f70/manobs_7e-a19_eng_web.pdf). As such, our analysis is based on statistics that include all nonzero precipitation
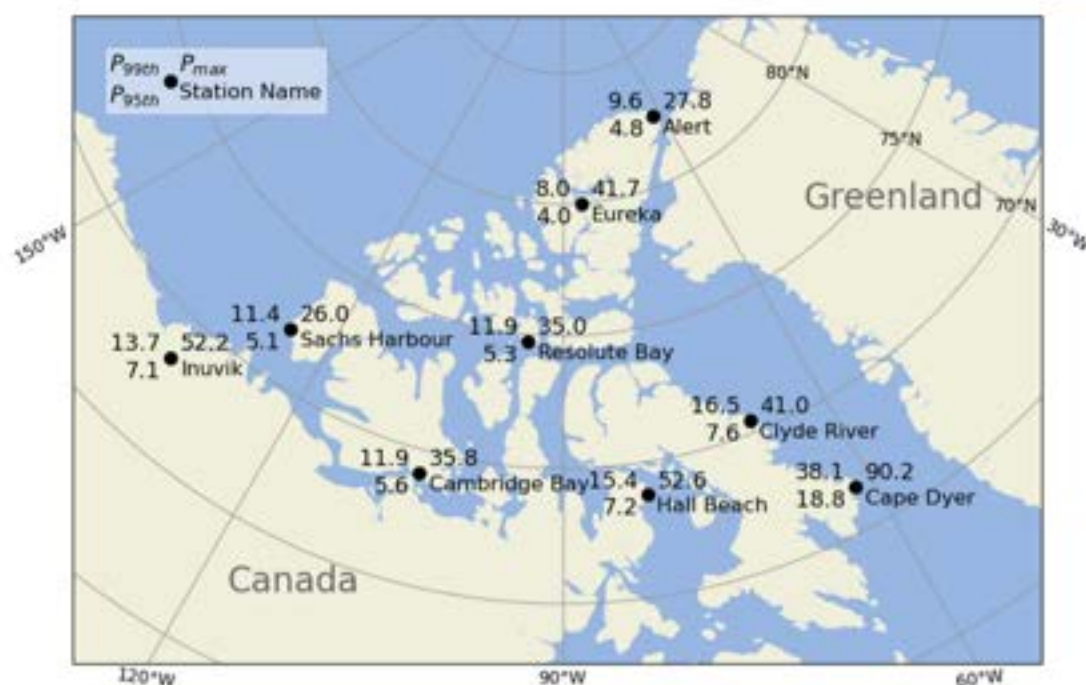
FIGURE 1 Location of the nine selected stations with long records, along with the sizes of the leading, 99th and 95th percentile events (in mm). Station elevations are given in Table 1

TABLE 1 Characteristics of the station records

Station	Latitude	Longitude	Elevation (m)	Start year	End year	% missing	Files used
Inuvik[a]	68.30	−133.48	68	1957	2006	2	INUVIK A
Sachs Harbour	71.99	−125.27	88	1955	2021	13	**SACHS HARBOUR A**, SACHS HARBOUR CLIMATE
Cambridge Bay[b]	69.11	−105.14	31	1929	2021	14	CAMBRIDGE BAY A (two files combined)
Resolute Bay	74.72	−94.97	68	1947	2021	1	**RESOLUTE CARS**, RESOLUTE BAY A
Alert	82.52	−62.28	30	1950	2021	1	**ALERT**, ALERT CLIMATE
Eureka	79.98	−85.93	10	1947	2021	1	**EUREKA A**, EUREKA CLIMATE
Hall Beach[c]	68.78	−81.24	9	1957	2021	7	HALL BEACH A (two files combined)
Clyde River[d]	70.49	−68.51	27	1933	2021	22	**CLYDE A**, CLYDE RIVER CLIMATE
Cape Dyer[e]	66.58	−61.62	393	1959	1993	3	CAPE DYER A

Note: In the case of stations with multiple records that were combined, the longest record (used as the base) is listed first in bold.

[a]INUVIK UA extends from 1995 to 2007; INUVIK CDA covers 1961 only.

[b]Three files listed under CAMBRIDGE BAY A, the longest runs from 1929 to 2015, the other two from 2015 and 2018 onwards. CAMBRIDGE BAY GSN runs from 2002 onwards.

[c]Two files listed under HALL BEACH A, the first from 1957 to 2014 and the second from 2012 to 2021.

[d]CLYDE RIVER A extends from 2013 to 2021; CLYDE AWOS, an automatic station, runs from 2008 to 2013.

[e]CAPE DYER contains 1958, then runs from 1993 onwards, but with no precipitation (assumed to be from an automated station).

events. Most Arctic precipitation events are quite small—for most of the stations studied here, more than 50% of daily precipitation totals are less than 1 mm (see later discussion). There are also many trace events with precipitation less than 0.2 mm. Trace events are considered "nonaccumulating" precipitation and are usually indicated by a "T" in the observational record, rather than an amount of accumulation.

2.2 | ERA5 atmospheric fields

To assess associated atmospheric conditions, reliance is placed on data from the ECMWF ERA5 atmospheric reanalysis (Hersbach et al., 2020; Bell et al., 2021). ERA5 data are available from 1950 onwards, but the quality of the output is more reliable starting in 1979, the start of the modern satellite era. Satellite data provide a wealth of information that may be assimilated into the analysis and forecasting system. The ERA5 data prior to 1979 is considered a "preliminary version," according to information provided on the Copernicus Climate Data website, where atmospheric reanalysis datasets can be obtained. ERA5 is the latest in what is now a long generation of atmospheric reanalysis efforts, and it performs slightly better than other atmospheric reanalyses at matching observed precipitation totals from extreme events in the eastern Canadian Arctic (Loeb et al., 2022).

ERA5 data are used in several ways. To assess the seasonality of extreme events, within the context of the mean seasonal cycles of precipitation at the different sites, use is made of fields of precipitable water (column integrated water vapour), 1,000–500 mb thickness and output from a cyclone detection and tracking algorithm applied to 3-hourly ERA5 sea level pressure (SLP) fields. SLP fields are regridded to a 25-km Lambert Azimuthal Equal-Area projection prior to applying the detection and tracking algorithm. The algorithm is described in detail by Crawford and Serreze (2016) and builds on the algorithm originally designed by Serreze (1995). It has been used by our group in studies that include cyclone response to the summer Arctic frontal zone (Crawford and Serreze, 2017) and the sensitivity of cyclone detection and tracking results to different temporal and spatial resolutions of input SLP fields (Crawford et al., 2021). Cyclone depth (the pressure at the edge of the storm minus the central pressure) is used as a metric of cyclone intensity/strength. To assess the meteorological conditions associated with the leading (largest) precipitation event at each station, and for the April 1977 case study, reliance is placed on ERA5 fields of SLP and the vertically integrated water vapour transport (IVT).

3 | EVENT MAGNITUDES

3.1 | Basic statistics

A precipitation event requires the availability of sufficient water vapour as well as a lifting mechanism (variously frontal uplift, low-level convergence, convection or orographic uplift) to cool air parcels to their dewpoint. While the basic precipitation statistics from the nine Canadian stations (Figure 1 and Table 2) document the general aridity of the Arctic environment—reflecting the air temperature control on the saturation vapour pressure—maritime influences are also prominent at some sites. The leading event sizes range from 90 mm at Cape Dyer (the southernmost station on the western side of Baffin Bay and the station with the highest elevation) to 26 mm at Sachs Harbour on the southwest coast of Banks Island. The 95th percentile events range from about 10 to 25% of the leading event sizes, from 19 mm at Cape Dyer to a paltry 4–8 mm at other sites. In turn, the 99th percentile events are only 20–50% of the leading events. As seen in Table 2 and at most of the sites, half of the precipitation events are less than 1 mm.

3.2 | Seasonality and marine influences

The preferred seasonal occurrence of extreme precipitation events should reflect the seasonality in available

TABLE 2 Percentile values of precipitation (mm) at the nine stations

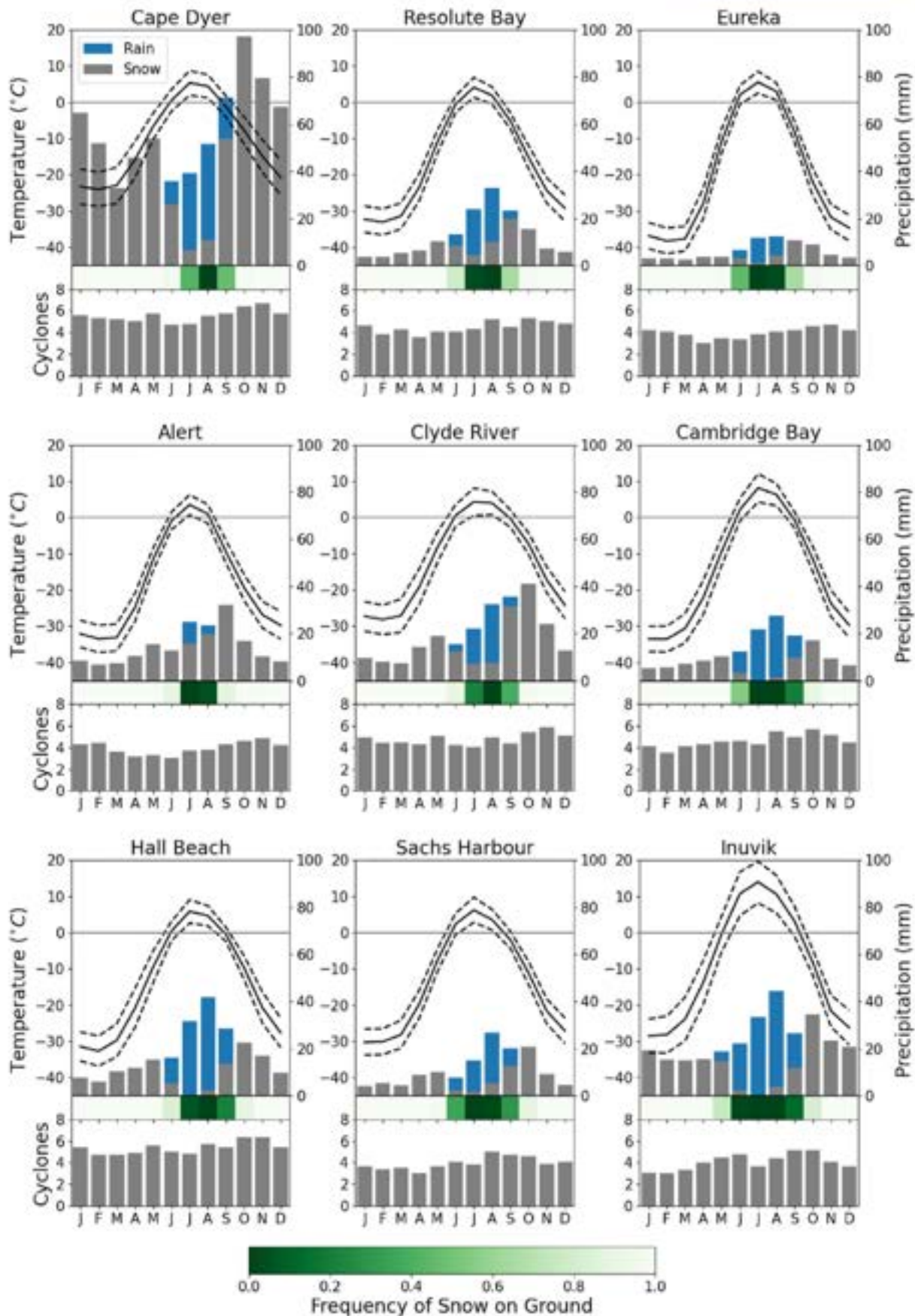| Station | Percentile (mm) | | | | | | | | | |
	1%	5%	10%	25%	50%	75%	90%	95%	99%	100%
Inuvik	0.2	0.2	0.3	0.5	1.0	2.2	4.6	7.1	13.7	52.2
Sachs Harbour	0.2	0.2	0.2	0.3	0.6	1.5	3.3	5.1	11.4	26.0
Cambridge Bay	0.2	0.2	0.2	0.3	0.6	1.5	3.6	5.6	11.9	35.8
Resolute Bay	0.2	0.2	0.2	0.3	0.6	1.5	3.3	5.3	11.9	35.0
Alert	0.2	0.2	0.2	0.4	0.7	1.5	3.3	4.8	9.6	27.8
Eureka	0.2	0.2	0.2	0.3	0.5	1.2	2.6	4.0	8.0	41.7
Hall Beach	0.2	0.2	0.2	0.4	0.8	2.2	4.8	7.2	15.4	52.6
Clyde River	0.2	0.2	0.2	0.4	0.9	2.3	5.0	7.6	16.5	41.0
Cape Dyer	0.2	0.2	0.3	0.5	1.6	5.1	12.2	18.8	38.1	90.2

FIGURE 2 Legend on next page.

TABLE 3 The fraction of daily total precipitation greater than the 95th percentile daily total precipitation falling in each month expressed as a percentage

| Station | 95th percentile events in each month as % | | | | | | | | | | | |
	Jan	Feb	Mar	Apr	May	Jun	Jul	Aug	Sep	Oct	Nov	Dec
Inuvik	2	1	0	2	9	12	19	**27**	9	8	3	2
Sachs Harbour	0	1	4	8	8	6	11	**30**	16	7	2	1
Cambridge Bay	0	0	0	1	2	9	24	**36**	16	7	1	0
Resolute Bay	0	0	0	1	2	9	24	**36**	16	6	1	0
Alert	1	0	0	3	6	8	27	20	**22**	6	2	2
Eureka	0	1	1	1	3	11	21	**24**	17	8	4	0
Hall Beach	0	1	3	2	4	7	20	**29**	16	7	3	1
Clyde River	1	1	1	4	6	8	12	20	18	**13**	8	4
Cape Dyer	9	7	2	4	4	4	4	9	12	**19**	10	9

Note: Fractions in the month of the climatological monthly precipitation maximum are in bold. Fractions have been rounded to the nearest integer.

water vapour and lifting mechanisms, which should also be expressed in the mean seasonal cycles of precipitation. At five of the nine stations, precipitation peaks in August (prime examples being Sachs Harbour and Resolute Bay), 1 month after peak precipitable water and the maximum surface air temperature (see later discussion) (Figure 2). Clyde River and Cape Dyer have October precipitation maxima. Alert has an overall summertime precipitation maximum. Eureka has a summer maximum but amounts are very small—this is the driest of the nine stations. However, consistent with earlier reasoning and at all locations, the frequency of the 95th percentile precipitation events is highest at or near the month of the seasonal precipitation maximum (Table 3). Looking back to Figure 2, even in mid-summer, some precipitation events represent snowfall.

In an earlier study, Serreze and Etringer (2003) used gauge data to examine the characteristics of precipitation averaged over the highly continental and moisture-limited major Arctic-draining Eurasian watersheds (The Ob, Yenisey, Lena). For each watershed they highlighted the existence of a distinct July precipitation maximum, coincident with the seasonal maximum in precipitable water (moisture availability) and surface air temperature. The largest events also tend to occur in July, with both convection and the summer peak in cyclone activity acting as moisture convergence and uplift mechanisms. This contrasts sharply with the Atlantic sector Arctic, in the vicinity of the Icelandic Low. Here, precipitation has a cold season maximum, reflecting the dominant roles of vapour flux convergence linked to frequent cyclone activity (Serreze and Etringer, 2003).

The different precipitation characteristics seen at the Canadian sites as compared to northern Eurasia can in turn be understood from the combination of marine influences and aspects of the large-scale atmospheric circulation. Marine influences are most obvious at Cape Dyer and Clyde River, where mean precipitation and the frequency of extremes peak in October. This follows in that these sites are exposed to the open water of Baffin Bay. In October, the overlying atmosphere is quite cool (Figure 2), implying high evaporation rates due to the lower atmospheric vapour pressure paired with the high saturation vapour pressure at the warmer open water surface. Similar effects are seen at Great Bear Lake in the Canadian Arctic and Lake Superior, where there are high late-season evaporation rates linked to the high heat capacity of the open water underlying a cool atmosphere (Blanken et al., 2000; 2011). At both Clyde River and Cape Dyer, sea ice typically forms in November, reducing the latent heat flux. This is consistent with the drop in mean precipitation and the frequency of extremes with respect to October.

The August precipitation peak seen at five of the stations appears to reflect more local marine influences (Hall Beach, Sachs Harbour, Inuvik, Cambridge Bay, Resolute Bay). The islands of Arctic Canada are interspersed with oceanic channels. While most of these are largely ice-covered in summer, they still provide a moisture source due to the availability of liquid water

FIGURE 2 Mean seasonal cycles of total precipitation (mm; total length of upper columns), divided into the amount of precipitation falling as snow (grey) and rain (blue), the daily maximum, minimum and mean temperature (°C; black lines), relative frequency of snow cover on the ground (green shading) and the mean number of cyclone passages (lower columns)
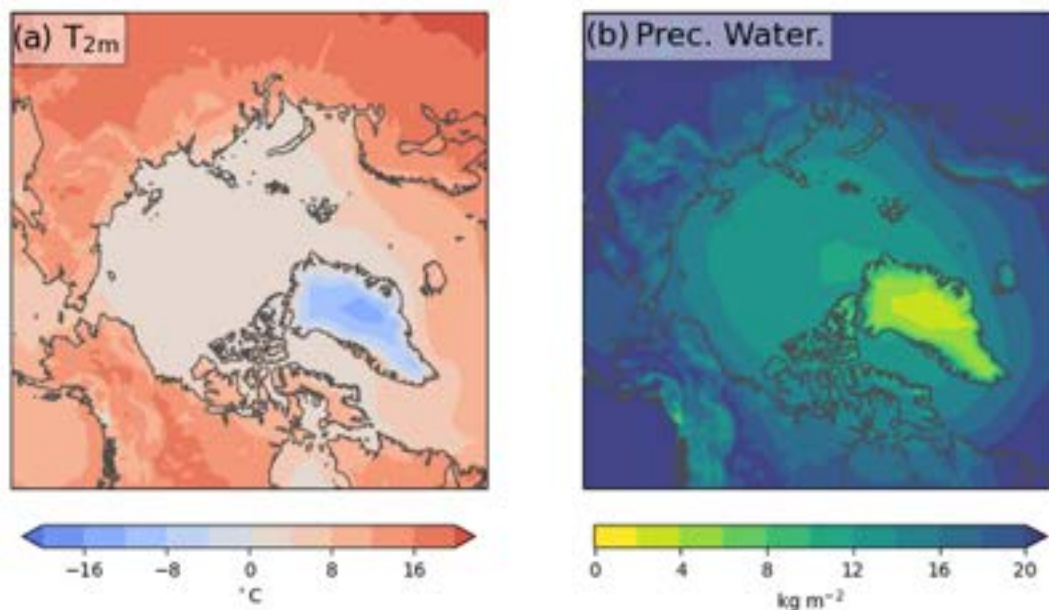
FIGURE 3 Average 2-m air temperature and precipitable water (kilograms per square meter, same as mm water depth) for July

on the sea ice surface. The effects of this surface moisture source will be prevalent in August, when the atmosphere begins to cool from its mid-summer peak. The exposed areas of melting ice or open water, coupled with the lower air temperatures, increases the vapour pressure gradient between the open water and lower atmosphere, thus enabling evaporation at a time when ample energy is still available. This helps to delay the seasonal precipitation peak (and the month of most frequent 95th percentile events) 1 month later compared to Eurasia. This effect is also apparent when comparing continental and more marine Canadian sites south of the Arctic Circle. For example, Thompson Manitoba has a July peak in precipitation, whereas Churchill Manitoba, which lies on the shore of Hudson Bay, has an August peak (not shown).

Marine influences, in concert with the overall colder summer climate of the Canadian Arctic Archipelago compared to the Eurasian watersheds, also tends to limit convective precipitation; this is consistent with the observations that summer precipitation overall is lower over the Canadian Arctic than over highly continental northern Eurasia (Serreze and Barry, 2014). As seen in Figure 3, the July seasonal peak in precipitable water is considerably lower over Arctic Canada than over northern Eurasia, and July surface air temperatures are also lower. These features are also consistent with the Canadian Arctic lying within a prominent trough in the tropospheric polar vortex, depicted in Figure 4 as the surface to 500 hPa thickness, which is a function of mean temperature in the low to middle troposphere.
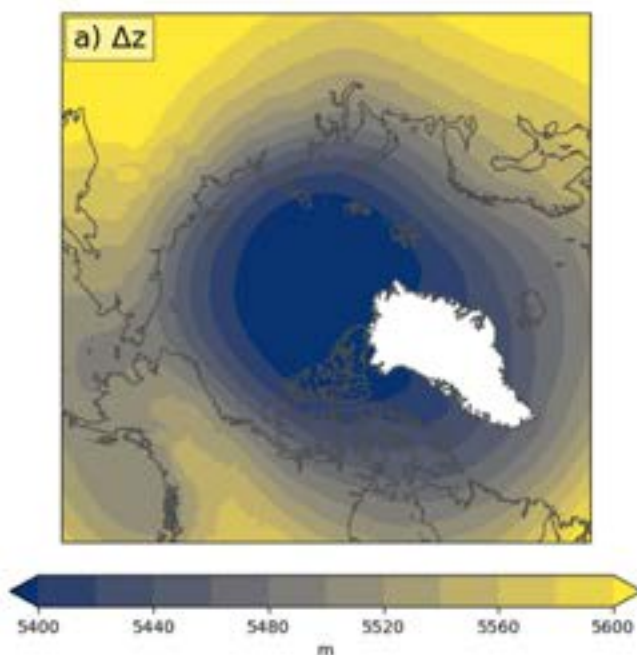

FIGURE 4 Mean surface to 500 mb thickness for July

3.3 | Influence of synoptic-scale cyclones

An obvious question that arises regarding Canadian Arctic precipitation is the role of cyclone activity as an uplift mechanism. Figure 2 shows by month the average number of cyclones passing within 800 km of each Canadian site. This recognizes that precipitation at a site can be influenced by cyclones centred a considerable distance from that site (e.g., the site could lie within the region of

frontal uplift of a cyclone centred well to the west). At most sites, the seasonal cycle in cyclone influence is fairly weak—stated differently, dynamic uplift mechanisms are common year-round. At several sites, including Clyde River and Cape Dyer, a slight annual peak occurs in November. Cyclone influences assessed for radii of 600 km or 1,000 km do not change the story.

To assess whether extreme precipitation events are more likely in the presence of synoptic-scale cyclones, especially when those cyclones are strong, we constructed two contingency tables for each station (Table 4). Contingency Table A is limited to days with nonzero precipitation and counts the number of extreme and nonextreme precipitation events, along with the number of precipitation days with or without a cyclone present within 800 km of the station. The 95th percentile is used to define "extreme." Contingency Table B is more limited: only days that have both nonzero precipitation and a cyclone present are considered. Precipitation events are again defined as extreme or nonextreme, but now they are compared to days for which a "weak" cyclone or "strong" cyclone was present. The 50th percentile of cyclone depth is used to distinguish cyclone categories.

These tables are summarized in two ways. First, we calculate the ratio difference (R) as $R = D/C - B/A$, where A–D are counts from the contingency tables. For Contingency Table A, a positive ratio difference indicates that extreme precipitation is more likely when a cyclone is present nearby (Table 5). For Contingency Table B, a positive ratio difference indicates that extreme precipitation is more likely when a strong cyclone (rather than weak cyclone) is present. Randomly distributed events would, on average, have a positive ratio difference of 0. To test the null hypothesis of no relationship between extreme precipitation and cyclone presence/strength, we use the likelihood ratio G-test (Cressie and Read, 1984).

Results of these tests show that extreme precipitation events are universally more common (a) when a cyclone is nearby compared and (b) when a nearby cyclone is stronger than the 50th percentile. In all but one case (presence/absence at Eureka), the distribution of events is significantly different from random chance at a 95% confidence level. However, storm intensity is just one notable factor; similar tables (not shown) comparing extreme storms (exceeding the 95th percentile) to nonextreme storms does not yield such clear results.

TABLE 4 Contingency tables for comparing counts of (non-)extreme precipitation events to (top) cyclone presence or absence and (bottom) the presence of weak (depth is below 50th percentile) or strong cyclones (depth exceeds 50th percentile) within 800 km of the station of interest

Contingency Table A	No nearby cyclone	Nearby cyclone
Nonextreme precipitation	A	B
Extreme precipitation	C	D
Contingency Table B	Weak cyclone	Strong cyclone
Nonextreme precipitation	A	B
Extreme precipitation	C	D

Note: "Extreme" is defined as exceeding the 95th percentile.

TABLE 5 Influence of (left) cyclone presence or (right) the presence of a strong versus weak cyclone with 800 km of each station on whether precipitation that occurs is extreme (exceeding the 95th percentile)

Station	Cyclone presence vs. absence		Strong vs. weak cyclone presence	
	Ratio difference	G statistic (p-value)	Ratio difference	G statistic (p-value)
Inuvik	3.04	47.06 (<.01)	3.04	17.58 (<.01)
Sachs Harbour	1.25	21.44 (<.01)	1.25	6.52 (.01)
Cambridge Bay	1.36	37.96 (<.01)	1.36	12.18 (<.01)
Resolute Bay	2.33	39.67 (<.01)	2.33	38.01 (<.01)
Alert	0.56	6.35 (.01)	0.56	18.10 (<.01)
Eureka	0.81	3.61 (.06)	0.81	17.88 (<.01)
Hall Beach	2.80	20.95 (<.01)	2.80	62.62 (<.01)
Clyde River	3.11	10.44 (<.01)	3.11	4.08 (.04)
Cape Dyer	2.32	25.69 (<.01)	2.32	91.10 (<.01)

Note: A positive ratio difference means that extreme precipitation is more likely if a cyclone is present (rather than absent), and when present, if a cyclone's depth exceeds the 50th percentile for that location.

4 | CHARACTERISTICS OF THE LEADING EVENTS

4.1 | Approach

While the frequency of 95th percentile events at each site corresponds broadly to (within a month of) the climatological monthly maximum precipitation, it is evident from Table 6 that this correspondence does not necessarily hold for the leading (largest) events in the records. As two outstanding examples, the leading events at Cape Dyer (90 mm) and Clyde River (41 mm) occurred in January and April, respectively, when Baffin Bay was completely ice-covered, cutting off the local moisture source. This implies a more remote moisture source. In turn, the leading event at Resolute Bay (35 mm) occurred in November—the mean precipitation for that month is only 6 mm. All of the unusual events that took place outside of the climatological monthly maximum precipitation, and outside of the expected maximum 95th percentile event frequency, fell as snow. Note that the leading event listed for Alert (28 mm) represents the second largest event in the Alert record. The largest reported event of 44 mm (April 6, 2008) was flagged by us as an obvious error, based both on the atmospheric pattern (which is entirely inconsistent with a precipitation event) and the very low temperatures of that day (a maximum of −22°C). Hence, we take the second largest event in the record, April 11, 2013, as the leading event.

Here, we examine the meteorological conditions associated with the leading event at each site. For events at eight of the sites, we plot the field of sea-level pressure and the vertically integrated water vapour transport (IVT) at the time of day that most clearly reflects the situation favouring precipitation. A more detailed assessment is first provided for Clyde River, where the leading single day event on April 7, 1977 was associated with a storm that first wreaked havoc across parts of the eastern United States. That was followed by a two-day event on April 27 (27 mm, third highest daily total in the record) and April 28 (38 mm, second highest daily total in the record). This led to a remarkable monthly total of 106 mm at Clyde River from the three storms, all precipitation falling as snow. While obtaining eyewitness accounts of April 1977 has so far been elusive, it can only be assumed that life in the community was greatly disrupted.

4.2 | Clyde River sequence

Six panels are used to illustrate the April 7, 1977 event as well as the April 27 and April 28 events. The April 7th event (Figure 5) began with a storm system that originated in northern Mexico and generated a severe weather outbreak across the southeastern United States before reaching the Canadian Arctic. This included tornadoes and significant hail, causing a major aircraft accident when hail was ingested into the engines of a DC-9 jet (The New York Times, 1977). This cyclone also produced flooding across parts of Kentucky, Tennessee, Virginia, and West Virginia (US Department of Commerce, 1977).

By April 6th, the storm system was a very deep low centred over southwestern Quebec (00Z panel) with strong moisture transport (maximum IVT values greater than 1,200 kg·m^{-1}·s^{-1}) spreading south to north along the US eastern seaboard. This cyclone then travelled north through Quebec, and the cyclone centre neared the southern tip of Baffin Island on the evening of April 6 (April 7 at 00Z). This moisture transport feature

TABLE 6 Date and size of the leading (largest) events

	Year	Month	Day	Size (mm)	Precipitation phase	Relative cyclone strength
Inuvik	1995	August	29	52	Not reported	72
Sachs Harbour	1990	April	26	26	Snow	87
Cambridge Bay	1988	July	24	36	Rain	93
Resolute Bay	2004	November	17	35	Snow	82
Alert	2013	April	11	28	Not reported	73
Eureka[a]	1953	August	17	42	Rain	41
Hall Beach	1980	August	27	53	Rain	81
Clyde River[b]	1977	April	7	41	Snow	42
Cape Dyer	1980	January	22	90	Snow	88

Note: Relative cyclone strength is the percentile of maximum cyclone depth for all storm passing within 800 km of the station.
[a]Very early in the record, atmospheric field suspect.
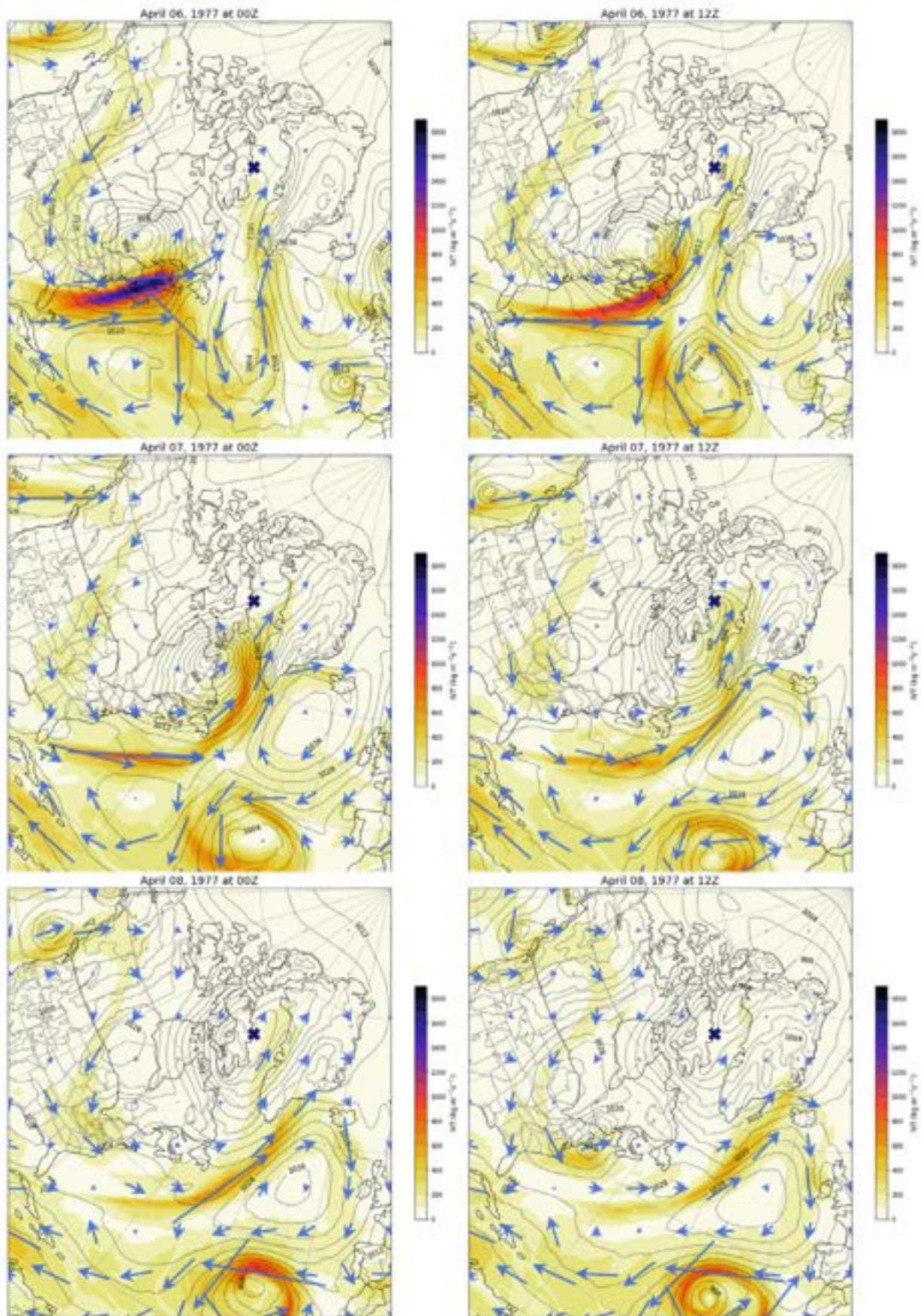[b]The three largest events in the Clyde River record were in April 1977.

FIGURE 5 Panels of MSLP contours, with IVT overlaid (as vectors and vector magnitudes), produced from ERA5 reanalysis data for April 6–8, 1977, for one of the Clyde River (dark blue "X") precipitation events
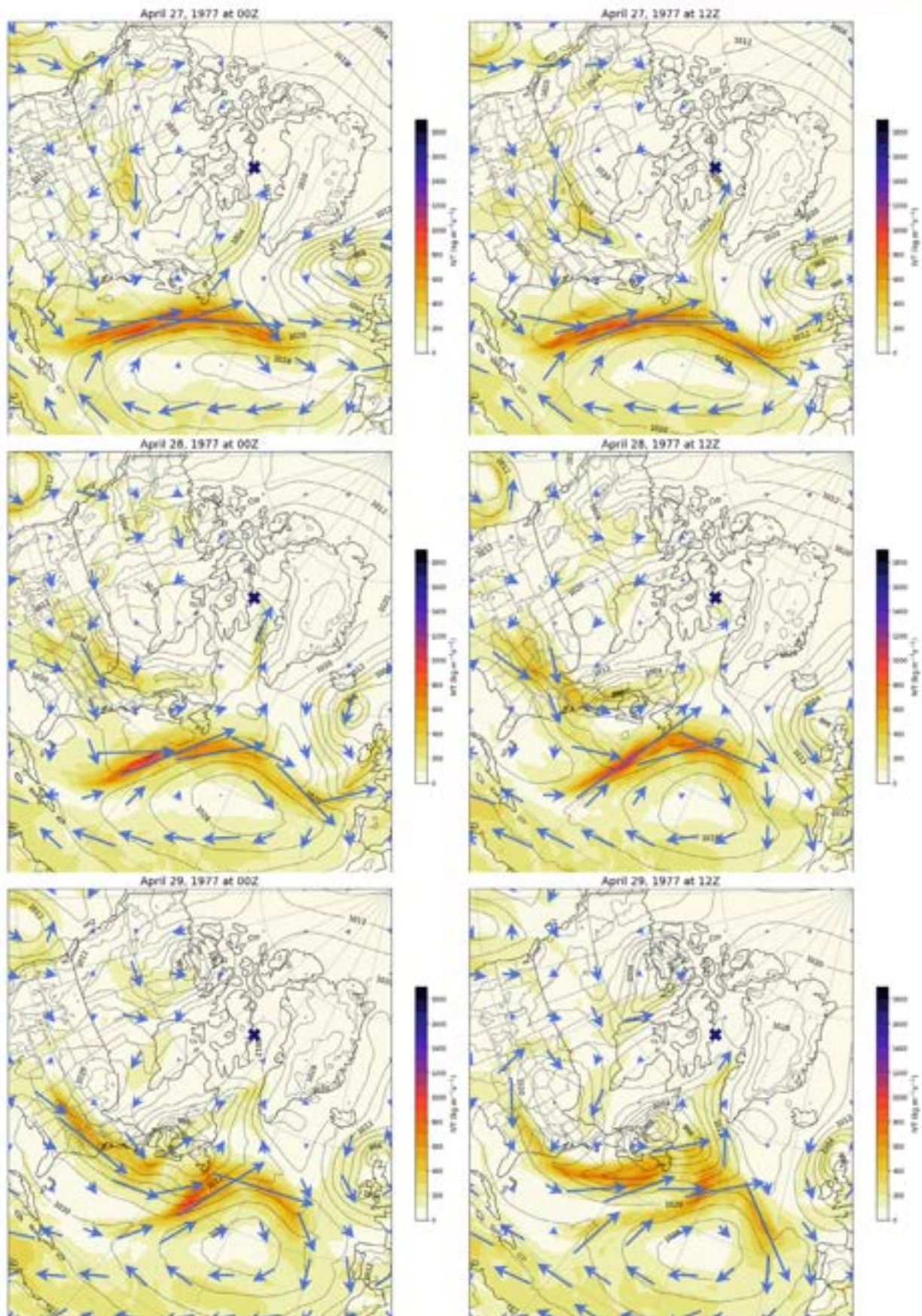
FIGURE 6 Panels of MSLP contours, with IVT overlaid (as vectors and vector magnitudes), produced from ERA5 reanalysis data for April 27–29, 1977, for one of the Clyde River (dark "X") precipitation events
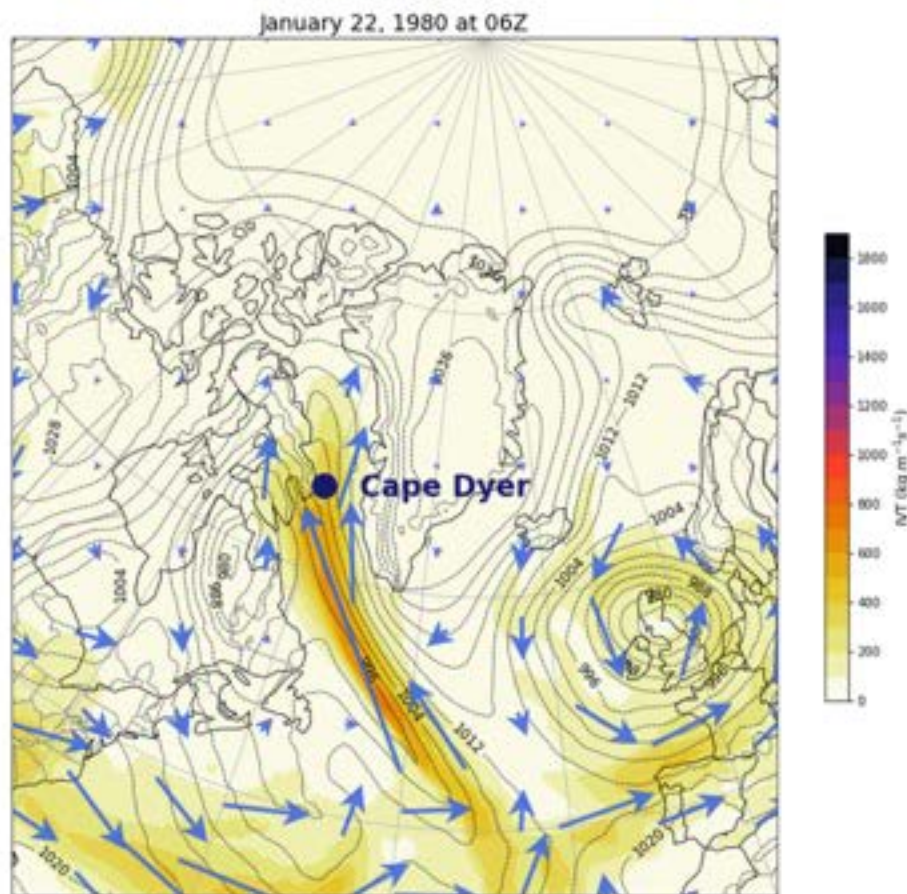
January 22, 1980 at 06Z

FIGURE 7 Image containing MSLP contours, with IVT overlaid (as vectors and vector magnitudes), produced from ERA5 reanalysis data for January 22, 1980, at 06Z for the Cape Dyer precipitation event

qualifies as an atmospheric river (AR), based on the $\geq$2,000-km length threshold of $\geq$250 kg·m^{-1}·s^{-1} IVT used in other AR studies (e.g., Rutz *et al.*, 2014). Given that Arctic temperatures are generally lower than in middle latitudes, limiting how much water vapour the atmosphere can carry, the threshold of what counts as an atmospheric river in the Arctic could arguably be set lower (e.g., Guan and Waliser, 2019). Note also that while our focus here is on IVT so as to easily identify moisture source regions and pathways, precipitation is more directly associated with the convergence of IVT than with the IVT magnitude itself (Benton and Estoque, 1954; Mo *et al.*, 2021).The cyclone then made its way to southern Baffin Island on April 7 (Figure 5, 00Z panel), enveloping a smaller system that was previously developing in Baffin Bay during April 6 (Figure 5, top panels) and reaching a central pressure of 980 hPa. IVT values remained elevated through Baffin Bay, with maximum values between 600 and 800 kg·m^{-1}·s^{-1}. Even as the system began to weaken on the April 7 (12Z) panel, IVT remained high between 200 and 400 kg·m^{-1}·s^{-1}. This strong cyclone led to the largest precipitation event ever recorded at Clyde River, with all of the precipitation falling as snow. With average wind speed exceeding 40 km·hr^{-1} for 16 hr on

April 7 and visibility as low as 0.0 km, this also developed into a strong blizzard.

The residents of Clyde River could not have foreseen what was to happen later in the month. The two-day Clyde River event of April 27 and 28 was associated with a low-pressure system that moved towards Baffin Island from the west, and then was directed north into Baffin Bay by a blocking pattern in the North Atlantic (Figure 6). This storm system, combined with a weaker area of low pressure over Quebec, led to a meridionally extensive area of cyclonic circulation. An AR seems likely in the North Atlantic, extending northeast just off the eastern seaboard of the United States and Canada on April 27 (12Z panel). Even though the enhanced moisture corridor flowed south of Baffin Island, enough moisture was stripped off and directed north with the low-pressure features to foster extreme precipitation. Most noticeable was the slightly elevated IVT (filled contours of 200–400 kg·m^{-1}·s^{-1}) moving north into Baffin Bay on the April 27 (12Z) and April 28 (00Z) panels. IVT vectors continued directing moisture towards the eastern edge of Baffin Island on the April 28 (12Z) panel. Again, all precipitation fell as snow, but this time it was accompanied by even stronger winds. Wind speeds exceeding

FIGURE 8   Image containing MSLP contours, with IVT overlaid (as vectors and vector magnitudes), produced from ERA5 reanalysis data for November 17, 2004, at 00Z for the Resolute Bay precipitation event
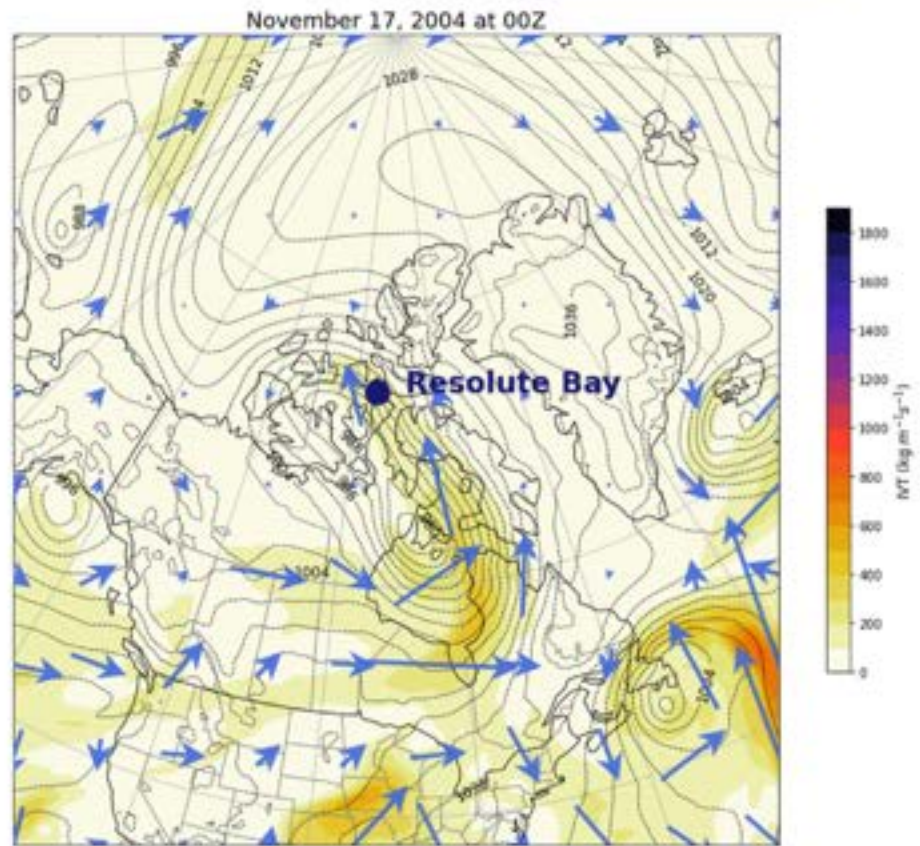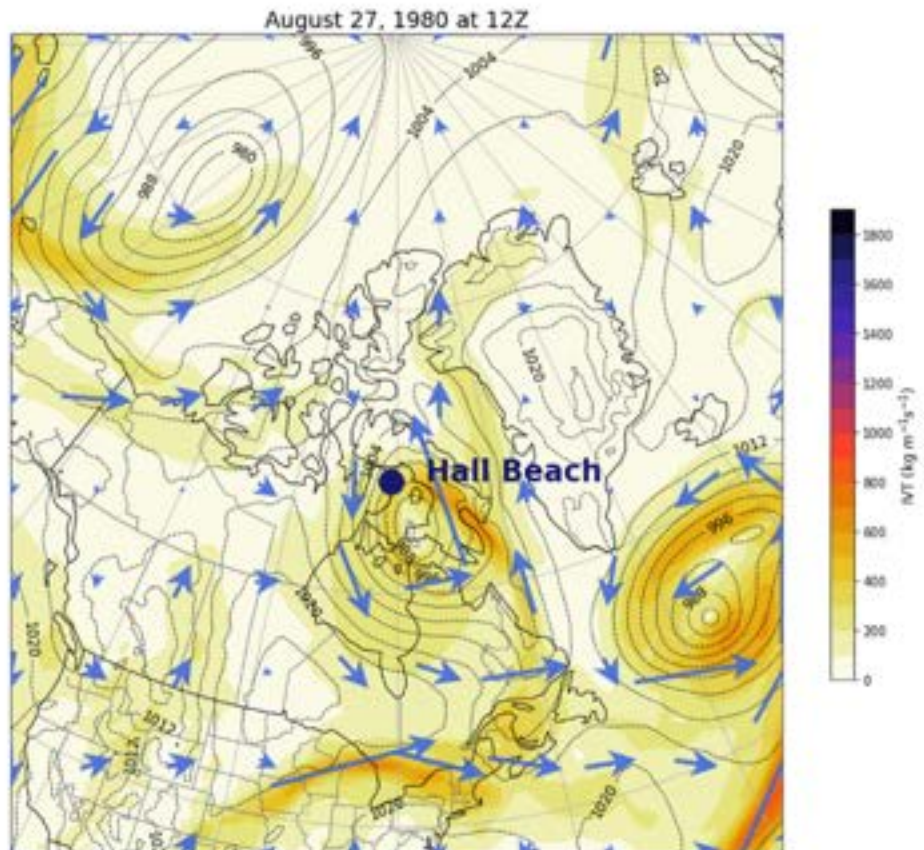

FIGURE 9   Image containing MSLP contours, with IVT overlaid (as vectors and vector magnitudes), produced from ERA5 reanalysis data for August 27, 1980, at 12Z for the Hall Beach precipitation event
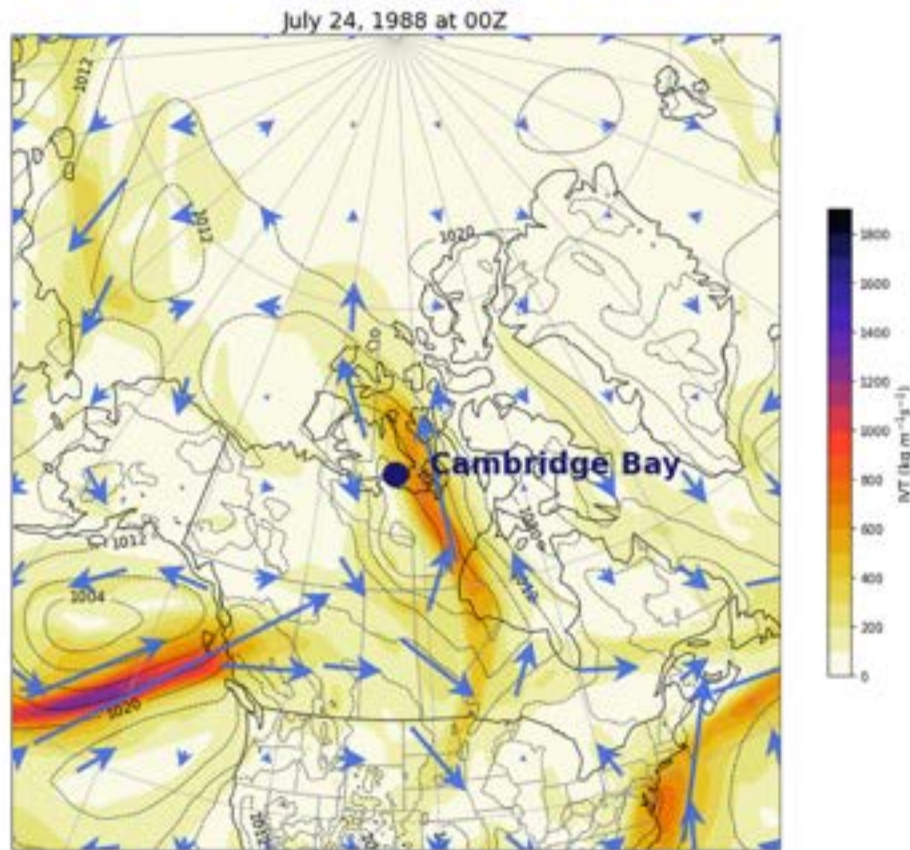
FIGURE 10 Image containing MSLP contours, with IVT overlaid (as vectors and vector magnitudes), produced from ERA5 reanalysis data for July 24, 1988, at 00Z for the Cambridge Bay precipitation event
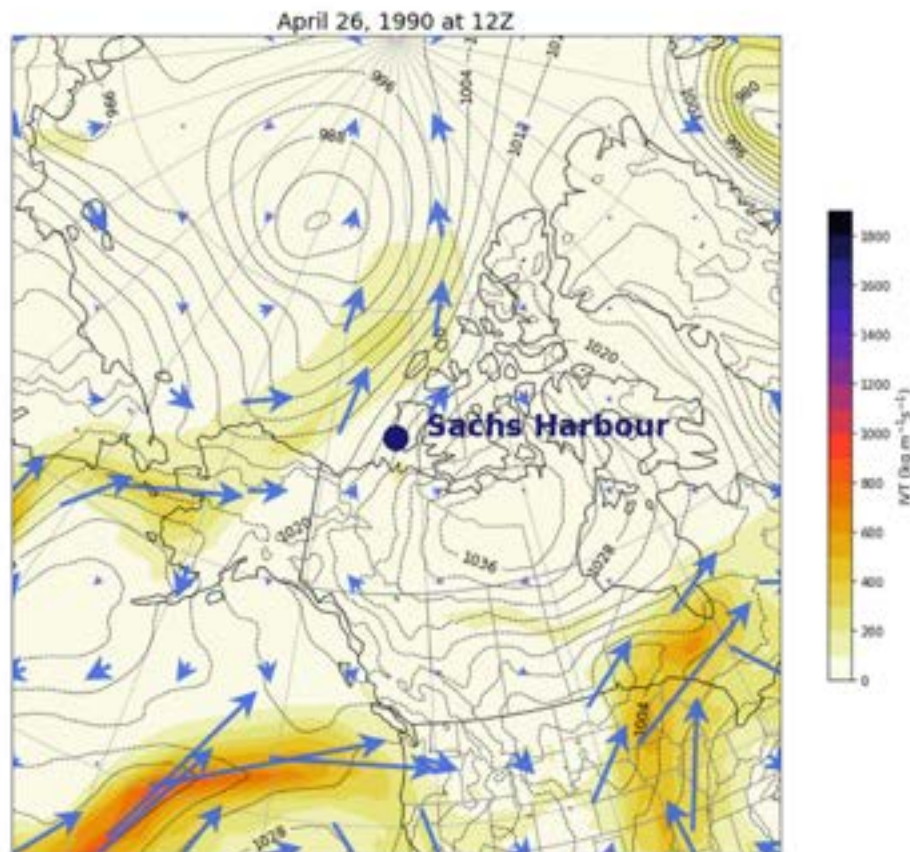

FIGURE 11 Image containing MSLP contours, with IVT overlaid (as vectors and vector magnitudes), produced from ERA5 reanalysis data for April 26, 1990, at 12Z for the Sachs Harbour precipitation event

FIGURE 12   Image containing MSLP contours, with IVT overlaid (as vectors and vector magnitudes), produced from ERA5 reanalysis data for August 29, 1995, at 18Z for the Inuvik precipitation event
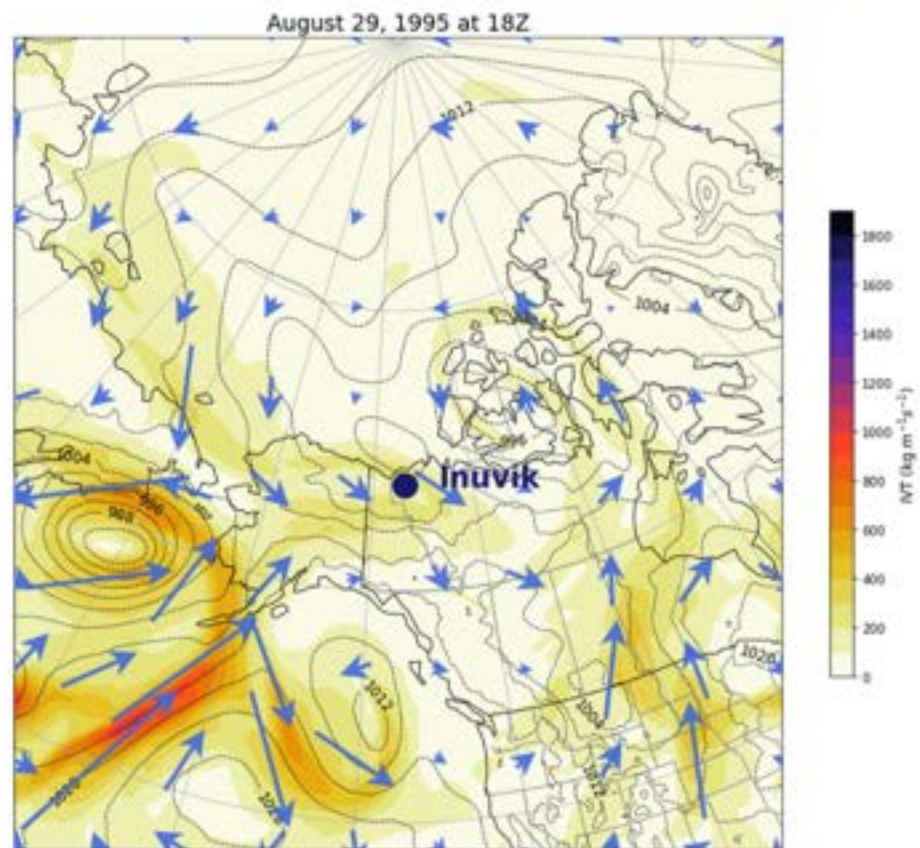
4.3 | Cape Dyer

Like Clyde River, Cape Dyer is situated on the east coast of Baffin Island. As such, it makes sense to examine this site next. One image was utilized that best represented the synoptic setup that led to the extreme precipitation event in this case. This same approach will be used for the remaining stations.

At 90 mm, the leading event at Cape Dyer, which occurred on January 22, 1980, is by far the largest of the nine stations. This event was associated with a cyclone that approached the region from the southeast. A storm system first formed off New England, headed northeast, then stalled on January 20. The cyclone then split up, one piece heading southeast and a second stronger piece diverging northwest towards northern Quebec. Similar to the Clyde River case on April 7, 1977, the situation on January 22 associated with the Cape Dyer event (Figure 7) featured an AR setup over the North Atlantic. However, the Cape Dyer case represented an instance of an AR making direct landfall, likely contributing to the extreme precipitation (which fell as snow). The AR on January 22 was associated with a blocking pattern. East of the deep cyclone on the northern edge of Quebec was a deep, high-pressure system over Greenland, with a closed low positioned over the United Kingdom and Ireland. The Canadian low and Greenland high, both abnormally deep, guided the AR to extend far north and made this case even more interesting because it occurred in one of the main winter months of January, when low air temperatures keep moisture availability low. Given the fairly high elevation of the Cape Dyer station (393 m, Table 1), it is reasonable to speculate that orographic uplift contributed to the already large size of this leading event.

4.4 | Resolute Bay, Hall Beach, and Cambridge Bay

These three sites lie largely in the central part of the Canadian Arctic Archipelago and are hence examined as a group. For all of these cases, an extratropical cyclone was likely the main contributor to the precipitation initiation. However, IVT values did not necessarily reach the criteria for an AR. The Resolute Bay event, occurring on
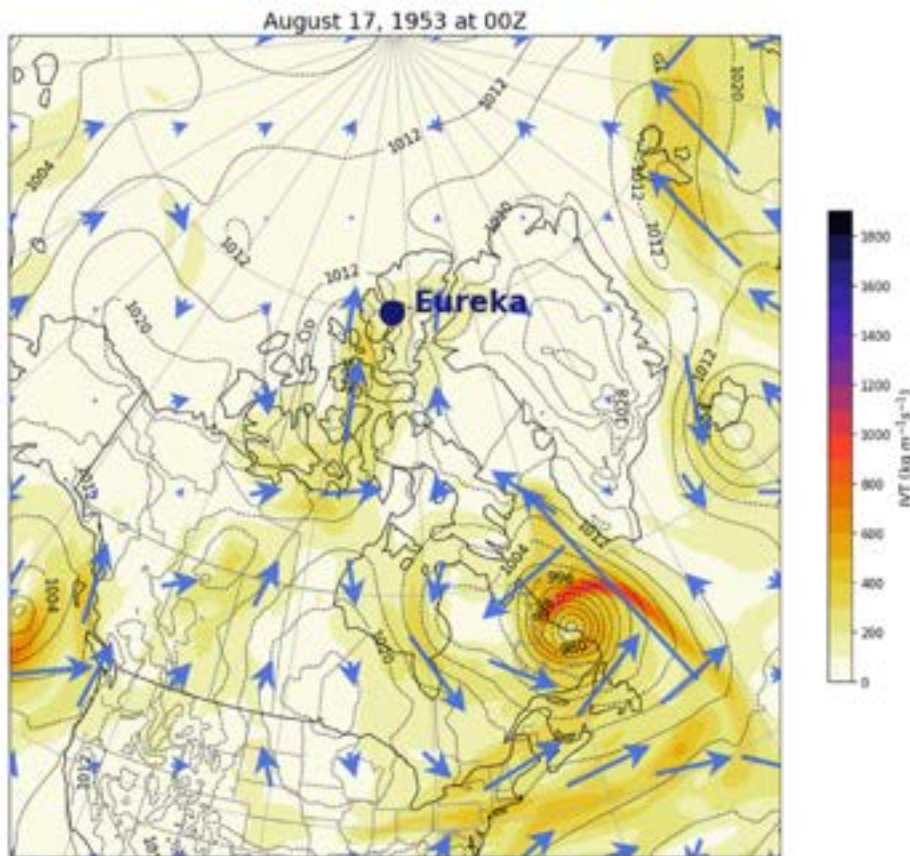
40 km·hr^{-1} persisted for 35 hr, and wind speeds over 50 km·hr^{-1} for 27 hr.

FIGURE 13 Image containing MSLP contours, with IVT overlaid (as vectors and vector magnitudes), produced from ERA5 reanalysis data for August 17, 1953, at 00Z for the Eureka precipitation event

November 17, 2004 (Figure 8), was linked to a multi-centre cyclone that stalled over Baffin Island after moving east from the Northern Rockies. Its elongated shape may have helped it tap into more southerly moisture sources. The Hall Beach case (rain) (Figure 9) occurred in August with higher temperatures, so there was more local water vapour available. This was also a notably strong storm system—the 87th percentile of cyclone depth for cyclones that come within 800 km of Hall Beach. The Cambridge Bay event (Figure 10) can be traced to a low-pressure area that originated in the lee of the Mackenzie range. By July 24, this low was centred over the northwestern edge of Nunavut. This storm attained a depth in the 93rd percentile for cyclones coming within 800 km of Cambridge Bay. It was able to draw a large area of high IVT from near Hudson Bay north into the location of interest. IVT values in the 600–800 kg·m^{-1}·s^{-1} range were located through the corridor of enhanced moisture transport. Since these high IVT values did not originate from a tropical or subtropical (or even maritime) source, this would not be considered a true AR. An AR was more likely present over the North Pacific, making landfall along the Canadian coast north of Vancouver Island, which may have supplied some of the moisture associated with the separate high IVT feature linked to the precipitation at Cambridge Bay.

4.5 | Sachs Harbour and Inuvik

These two stations are grouped together as being the westernmost stations in the Canadian Arctic Archipelago. The Sachs Harbour case on April 26, 1990 (snow) is intriguing, since the associated cyclone crossed over the ice-covered Arctic Ocean (Figure 11). Therefore, the moisture source was likely more remote, such as the IVT maximum associated with the storm passing near Kamchatka and through the Bering Strait, that is, a Pacific source. Looking at the August 29, 1995 Inuvik case (Figure 12), an AR-like feature was present over the North Pacific, linked to the combination of a deep cyclone centred over the Bering Sea and a strong Pacific high (an eggbeater effect). Enhanced moisture transport took place along the pressure gradient between these two features, with IVT values maxing out between 1,000–1,200 kg·m^{-1}·s^{-1} at 12Z on August 29. Precipitation that initiated over Inuvik seems to be associated with the small low positioned just to the north of the location of interest. While seemingly weak (18 hPa depth), this storm system actually ranks in the 72nd percentile of strength for cyclones within 800 km of Inuvik. Therefore, in a relative sense, uplift dynamics were likely fairly strong for this region. The deeper system over Banks Island had been swirling around the Canadian Arctic

FIGURE 14 Image containing MSLP contours, with IVT overlaid (as vectors and vector magnitudes), produced from ERA5 reanalysis data for April 12, 2013, at 00Z for the Alert precipitation event
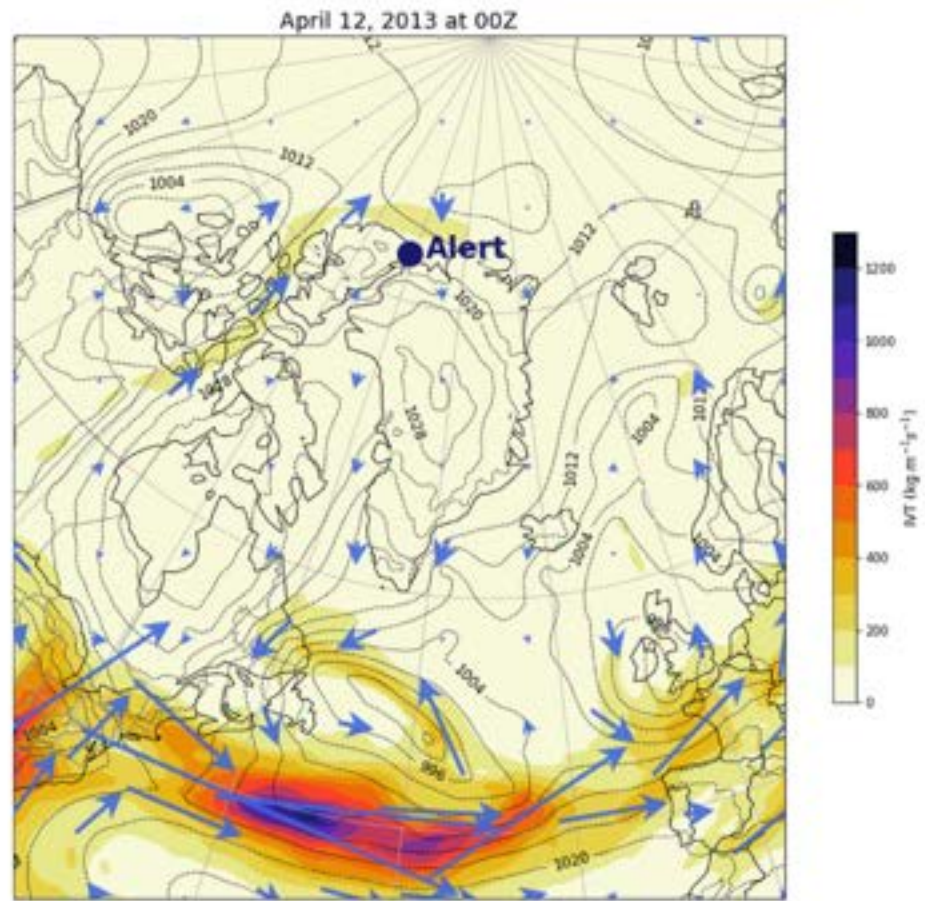
Archipelago for several days without causing notable precipitation, but then this small system barrelled in from the west, dragging moisture with it.

4.6 | Eureka and Alert

Eureka and Alert are the most northerly of the two sites and furthest removed from significant oceanic moisture sources from the Atlantic or Pacific. Because it occurred early in the ERA5 record (August 17, 1953), the meteorological setup associated with the Eureka leading event should be viewed with appropriate caution; the results in Figure 13 nevertheless serve to illustrate the effects of this strong continentality. The event was associated with a weak cyclone (maximum depth of 10 hPa) centred over the northwestern part of the Canadian Arctic Archipelago, which split off from a storm system that had stalled in the Gulf of Alaska. While IVT values on the east side of the low, associated with flow from the south, were elevated around the Eureka site compared to the surroundings, values are modest—this was clearly not an AR. There was some suggestion that the elevated IVT was a remnant of an AR that used to extend from the Pacific—associated with a stronger, stalled cyclone in the

Gulf of Alaska. Note from Table 6 that this August event fell as rain.

The Alert case on April 11, 2013 (Figure 14) was associated with a similarly weak low-pressure system, but centred further west, just north of Banks Island, and with a notably weak moisture flow. IVT values between 100 and 200 kg·m^{-1}·s^{-1} are seen extending from just northwest of Hudson Bay to the northernmost tip of Ellesmere Island. Moisture likely travelled with this weak cyclone from when it had originated as a deeper cyclone over the Gulf of Alaska several days earlier. While not reported, this was presumably a snow event.

5 | DISCUSSION AND CONCLUSIONS

Apart from perhaps Cape Dyer, the size of the leading events at the Canadian sites examined here would merit little attention in areas such as the Atlantic seaboard of North America, where moisture is abundant and strong winter cyclones associated with the North Atlantic cyclone track are common. But, as noted in the introduction, extreme precipitation events in the Arctic, albeit

comparably small, can have significant effects on physical, biotic, and human systems. While first-hand accounts of the remarkable series of three major events in April 1977 at Clyde River (the three largest events in the precipitation records) are at present lacking, it can only be assumed that they caused great disruption at this small and isolated Inuit community, especially because the associated high winds would have caused extensive drifting.

Although not surprising, while the frequency of 95th percentile precipitation events at the nine sites examined tends to be greatest during or near the month of maximum mean precipitation, the leading events can occur at any time of year, even when the background climate conditions seem unfavourable. The best example of this was at Cape Dyer, where the leading event occurred when Baffin Bay, a significant local moisture source, was iced over. The leading events at each site were associated with unique synoptic-scale setups. Extreme events were generally more likely when cyclones (especially strong cyclones) were present, and most, but not all, leading events were associated with relatively strong cyclones. In one of the cases, the April 7 event at Clyde River, the cyclone associated with the event could be clearly traced back to the southern United States, where it left a path of destruction as it made its way north. However, the common thread between the events, apart from the two highest latitude sites of Alert and Eureka, was significant moisture transport, in some cases directly associated with atmospheric rivers. The recent effort by Voveris (2022), which focuses on Arctic rain-on-snow events with known significant impacts, also shows a clear association between these events and direct or indirect influences of atmospheric rivers. Not studied here but meriting further analysis is the importance of moisture advection against local topography (e.g., Gilsan and Gutowski Jr., 2014), such as what we speculate contributed to the especially large (90 mm) leading event at Cape Dyer. Given the impacts of Arctic precipitation extremes, northern communities will benefit from improved forecasting of the features identified here as of key importance, notably, blocking situations, strong cyclones, the evolution of atmospheric rivers and local topography. For example, several days advance warning might be sufficient for reindeer herders to organize for supplemental feeding of their animals.

As noted in the introduction, while the observational evidence for systematic trends in Arctic precipitation and precipitation extremes is spotty (Walsh et al., 2020; Yu and Zhong, 2021), results from numerous modelling studies point to a future Arctic with more precipitation, a transition from snowfall- to rainfall-dominated climates, and a shorter return period for high-intensity events (e.g., Kharin et al., 2013; Sillmann et al., 2013; Toreti et al., 2013; Kusunoki et al., 2015; McCrystall et al., 2021). Given that these high-intensity events pose the greatest threats to Arctic ecosystems, the built environment, and human activities and that significant infrastructure gaps and vulnerabilities exist in the Canadian Arctic (Canadian Climate Institute, 2022), a focus on the characteristics of extreme events—and the apparent mismatch between observations and model projections—should also be a high research priority.

ORCID

Mark C. Serreze https://orcid.org/0000-0001-7670-0140

REFERENCES

Bell, B., Hersbach, H., Simmons, A., Berrisford, P., Dahlgren, P., Horányi, A., Muñoz-Sabater, J., Nicolas, J., Radu, R., Schepers, D., Soci, C., Villaume, S., Bidlot, J.-R., Haimberger, L., Woollen, J., Buontempo, C., and Thépaut, J.-N. (2021) The ERA5 global reanalysis: preliminary extension to 1950. Quarterly Journal of the Royal Meteorological Society, 147, 4186–4227. https://doi.org/10.1002/qj.4174.

Benton, G.S. and Estoque, M.A. (1954) Water-vapor transfer over the North American continent. Journal of Meteorology, 11, 462–477. https://doi.org/10.1175/1520-0469(1954)011<0462:WVTOTN>2.0.CO;2.

Bjerke, J.W., Tømmervik, H., Zielke, M. and Jørgensen, M. (2015) Impacts of snow season on ground-ice accumulation, soil frost and primary productivity in a grassland of sub-Arctic Norway. Environmental Research Letters, 10, 095007. https://doi.org/10.1007/s13280-016-0770-0.

Blanken, P.D., Rouse, W.R., Culf, A.D., Spence, C., Boudreau, L.D., Jasper, J.N., Kochtubajda, B., Schertzer, W.M., Marsh, P. and Verseghy, D. (2000) Eddy covariance measurements of evaporation from Great Slave Lake. Northwest Territories. Canada Water Resources Research, 36, 1069–1077. https://doi.org/10.1029/1999WR900338.

Blanken, P.D., Spence, C., Hedstrom, N. and Lenters, J.D. (2011) Evaporation from Lake Superior: 1. Physical controls and processes. Journal of Great Lakes Research, 37, 707–716. https://doi.org/10.1016/j.jglr.2011.08.009.

Canadian Climate Institute. (2022) Due North: Facing the Costs of Climate Change for Northern Infrastructure. Ottawa, ON: Canadian Climate Institute. Available at: https://climateinstitute.ca/wp-content/uploads/2022/06/Due-North.pdf.

Crawford, A.D., Schreiber, E.P., Sommer, N., Serreze, M.C., Stroeve, J.C., and Barber, D.G. (2021) Sensitivity of Northern Hemisphere cyclone detection and tracking results to fine spatial and temporal resolution using ERA5. Journal of Climate, 149, 2581–2598. https://doi.org/10.1175/MWR-D-20-0417.1.

Crawford, A.D. and Serreze, M.C. (2016) Does the summer Arctic frontal zone influence Arctic Ocean cyclone activity? Journal of

Climate, 29, 4977–4993. https://doi.org/10.1175/JCLI-D-15-0755.1.

Crawford, A.D. and Serreze, M.C. (2017) Projected changes in the Arctic frontal zone and summer Arctic cyclone activity in the CESM large ensemble. Journal of Climate, 30, 9847–9869. https://doi.org/10.1175/JCLI-D-17-0296.1.

Cressie, N. and Read, T.R.C. (1984) Multinomial goodness-of-fit tests. Journal of the Royal Statistical Society: Series B, 46, 440–464.

Dou, T.F., Pan, S.F., Binjanta, R. and Xiao, C.D. (2022) More frequent, intense, and extensive rainfall events in a strongly warming Arctic. Journal of Geophysical Research: Earth's Future, 10, e2021EF002378. https://doi.org/10.1029/2021EF002378.

Doyle, S.H., Hubbard, A., van de Wal, R.S.W., Box, J.E., van As, D., Scharrer, K., Meierbachtol, T.W., Smeets, P.C.J.P., Harper, J.T., Johansson, E., Mottram, R.H., Mikkelsen, A.B., Wilhelms, F., Patton, H., Christoffersen, P. and Hubbard, B. (2015) Amplified melt and flow of the Greenland ice sheet driven by late-summer cyclonic rainfall. Nature Geoscience, 8, 647–653. https://doi.org/10.1038/ngeo2482.

Forbes, B.C., Kumpula, T., Meschyb, N., Laptander, R., Macias-Fauria, M., Voveris, J., Stroeve, J., Sheffield, B., Forbes, B.C., Rasmus, S., Laptander, R., Brook, M., Brubaker, M., Temte, M., McCrystal, M., and Bartsch, A. (2016) Sea ice, rain-on-snow and tundra reindeer nomadism in Arctic Russia. Biology Letters, 12, 20160466. https://doi.org/10.1096/rsbl2016.0466.

Gilsan, J.M. and Gutowski, W.J., Jr. (2014) WRF summer extreme daily precipitation over the CORDEX Arctic. Journal of Geophysical Research: Atmospheres, 119, 1720–1732. https://doi.org/10.1002/2013JD020697/.

Guan, B. and Waliser, D.E. (2019) Tracking atmospheric rivers globally: spatial distributions and temporal evolution of life cycle characteristics. Journal of Geophysical Research: Atmospheres, 124, 12523–12552. https://doi.org/10.1029/2019JD031205.

Hansen, B.B., Isaksen, K., Benestad, R.E., Kohler, J., Pedersen, A.Ø., Loe, L.E., Coulson, S.J., Larsen, J.O., and Varpe, Ø. (2014) Warmer and wetter winters: characteristics and implications of an extreme weather event in the High Arctic. Environmental Research Letters, 9, 114021. https://doi.org/10.1088/1748-9326/9/11/114021.

Hersbach, H., Bell, B., Berrisford, P., Hirahara, S., Horanyi, A., Muñoz-Sabater, J., Nicolas, J., Peubey, C., Radu, R., Schepers, D., Simmons, A., Soci, C., Abdalla, S., Abellan, X., Balsamo, G., Bechtold, P., Biavati, G., Bidlot, J., Bonavita, M., De Chiara, G., Dahlgren, P., Dee, D., Diamantakis, M., Dragani, R., Flemming, J., Forbes, R., Fuentes, M., Geer, A., Haimberger, L., Healy, S., Hogan, R.J., Hólm, E., Janisková, M., Keeley, S., Laloyaux, P., Lopez, P., Lupu, C., Radnoti, G., de Rosnay, P., Rozum, I., Vamborg, F., Villaume, S., and Thépaut, J.N. (2020) The ERA5 global reanalysis. Quarterly Journal of the Royal Meteorological Society, 146, 1999–2049. https://doi.org/10.1002/qj.3803.

Kharin, V.V., Zwiers, F.W., Zhang, X. and Wehner, M. (2013) Changes in temperature and precipitation extremes in the CMIP5 ensemble. Climatic Change, 119, 345–357. https://doi.org/10.1007/s10584-013-0705-8.

Kusunoki, S., Mizuta, R. and Hosaka, M. (2015) Future changes in precipitation intensity over the Arctic projected by a global atmospheric model with a 60-km grid size. Polar Science, 9, 277–292. https://doi.org/10.1016/j.polar.2015.08.001.

Loeb, N.A., Crawford, A., Stroeve, J.C. and Hanesiak, J. (2022) Extreme precipitation in the eastern Canadian Arctic and Greenland: an evaluation of atmospheric reanalyses. Frontiers in Environmental Science, 10. https://doi.org/10.3389/fenvs.2022.866929.

McCrystall, M., Stroeve, J., Serreze, M.C., Forbes, B.C. and Screen, J. (2021) New climate models reveal faster and larger increases in Arctic precipitation than previously projected. Nature Communications, 12, 6765. https://doi.org/10.1038/s41467-021-27031-y.

Mo, R., So, R., Brugman, M.M., Mooney, C., Liu, A.Q., Jakob, M., Castellan, A. and Vingarzan, V. (2021) Column relative humidity and primary condensation rate as two useful supplements to atmospheric river analysis. Water Resources Research, 57, e2021WR029678. https://doi.org/10.1029/2021WR029678.

Ralph, F.M., Dettinger, M., Lavers, D., Gorodetskaya, I.V., Martin, A., Viale, M., White, A.B., Oakley, N., Rutz, J., Spackman, J.R., Wernli, H. and Cordeira, J. (2017) Atmospheric rivers emerge as a global science and applications focus. Bulletin of the American Meteorological Society, 98, 1969–1973. https://doi.org/10.1175/BAMS-D-16-0262.1.

Ralph, F.M. and Dettinger, M.D. (2011) Storms, floods, and the science of atmospheric rivers. Eos, Transactions American Geophysical Union, 92, 265–266. https://doi.org/10.1029/2011EO320001.

Rennert, K.J., Roe, G., Putkonen, J. and Bitz, C.M. (2009) Soil thermal and ecological impacts of rain on snow events in the circumpolar Arctic. Journal of Climate, 22, 2302–2315. https://doi.org/10.1175/2008JCLI2117.1.

Rutz, J.J., Steenburgh, W.J. and Ralph, F.M. (2014) Climatological characteristics of atmospheric rivers and their inland penetration over the western United States. Monthly Weather Review, 142, 905–921. https://doi.org/10.1175/MWR-D-13-00168.1.

Scheller, J., Scheel, M., Jackowicz-Korczynski, M., Langley K., Murphy, M.J. and Mastepanov, M. et al. (2021) Multiple ecosystem effects of extreme weather events in the Arctic. Ecosystems, 24, 122–136. https://doi.org/10.1007/s10021-020-00507-6.

Serreze, M.C. (1995) Climatological aspects of cyclone development and decay in the Arctic. Atmos.–Ocean, 33, 1–23. https://doi.org/10.1080/07055900.1995.9649522.

Serreze, M.C. and Barry, R.G. (2014) The Arctic Climate System, 2nd edition. Cambridge: Cambridge University Press, 404 pp.

Serreze, M.C., Crawford, A. and Barrett, A.P. (2015) Extreme daily precipitation events at Spitsbergen, an Arctic Island. International Journal of Climatology., 35, 4574–4588. https://doi.org/10.1002/joc.4308.

Serreze, M.C. and Etringer, A.J. (2003) Precipitation characteristics of the Eurasian Arctic drainage system. International Journal of Climatology, 23, 1267–1291. https://doi.org/10.1002/joc.941.

Serreze, M.C., Gustavson, J., Barrett, A.P., Druckenmiller, M.L., Fox, S., Voveris, J., Stroeve, J., Sheffield, B., Forbes, B.C., Rasmus, S., Laptander, R., Brook, M., Brubaker, M., Temte, M., McCrystal, M., and Bartsch, A. (2021) Arctic rain on snow events: bridging observations to understand environmental and livelihood impacts. Environmental Research Letters, 16, 105009. https://doi.org/10.1088/1748-9326/ac269b.

Sillmann, J., Kharin, V.V., Zwiers, F.W., Zhang, X. and Bronaugh, D. (2013) Climate extremes indices in the CMIP5

multimodel ensemble: Part 2. Future climate projections. *Journal of Geophysical Research: Atmospheres*, 118, 2473–2493. https://doi.org/10.1002/jgrd.50188.

The New York Times. (1977) *Hail in engines is blamed in Georgia crash killing 68*. The New York Times, April 6, 1977. Available at: https://www.nytimes.com/1977/04/06/archives/hail-in-engines-is-blamed-in-georgia-crash-killing-68.html.

Toreti, A., Naveau, P., Zampieri, M., Schindler, A., Scoccimarro, E., Xoplaki, E., Dijkstra, H.A., Gualdi, S. and Luterbacher, J.J. (2013) Projections of global changes in precipitation extremes from coupled model intercomparison project phase 5 models. *Geophysical Research Letters*, 40, 48887–48892. https://doi.org/10.1002/grl.50940.

US Department of Commerce, NOAA. (1977) *The East Kentucky Flood of April 1977*. NOAA's National Weather Service. Available at: https://www.weather.gov/jkl/1977flood [Accessed 17th February 2022].

Voveris, J. (2022) *Meteorological drivers of arctic rain on snow events and how climate change may influence associated risks*. Master's thesis, Department of Geography University of Colorado, Boulder, CO, 153 pp.

Walsh, J.E., Ballinger, T.J., Euskirchen, E.S., Hanna, E., Mård, J., Overland, J.E., Tangen, H. and Vihma, T. (2020) Extreme weather and climate events in northern areas: a review. *Earth-Science Reviews*, 209, 103324. https://doi.org/10.1016/j.earscirev.2020.103324.

Yu, L. and Zhong, S. (2021) Trends in Arctic seasonal and extreme precipitation in recent decades. *Theoretical and Applied Climatology*, 145, 1541–1559. https://doi.org/10.21203/rs.3.rs-385100/v1.

How to cite this article: Serreze, M. C., Voveris, J., Barrett, A. P., Fox, S., Blanken, P. D., & Crawford, A. (2022). Characteristics of extreme daily precipitation events over the Canadian Arctic. *International Journal of Climatology*, 1–20. https://doi.org/10.1002/joc.7907